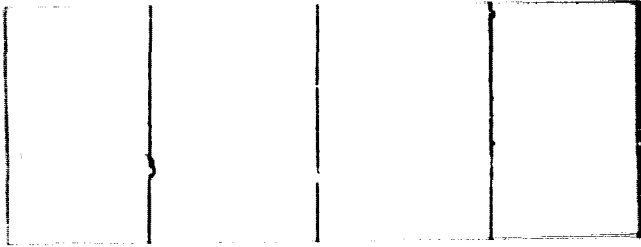


General Disclaimer

One or more of the Following Statements may affect this Document

- This document has been reproduced from the best copy furnished by the organizational source. It is being released in the interest of making available as much information as possible.
- This document may contain data, which exceeds the sheet parameters. It was furnished in this condition by the organizational source and is the best copy available.
- This document may contain tone-on-tone or color graphs, charts and/or pictures, which have been reproduced in black and white.
- This document is paginated as submitted by the original source.
- Portions of this document are not fully legible due to the historical nature of some of the material. However, it is the best reproduction available from the original submission.



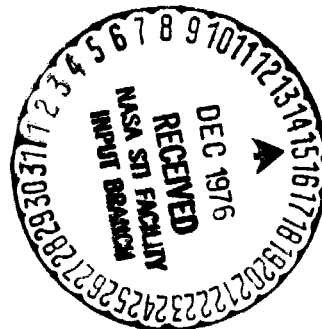
(NASA-CR-150107) VIGNETTING CHARACTERISTICS
OF THE S-056 X-RAY TELESCOPE Final Report
(Montevallo Research Associates, Ala.) 21 p
HC A02/MF A01 CSCL 20F

N77-12859

Unclas
56563

G3/74

**MONTEVALLO
RESEARCH
ASSOCIATES**



MAY 13 1975

Vignetting Characteristics of the
S-056 X-Ray Telescope

Contract No. NAS8-31996

FINAL REPORT

by

J. William Foreman, Jr.

Joseph M. Cardone

April, 1976

Submitted to

National Aeronautics and Space Administration
George C. Marshall Space Flight Center
Huntsville, Alabama

by

MONTEVALLO RESEARCH ASSOCIATES
Montevallo, Alabama

TABLE OF CONTENTS

	<u>Page</u>
I. INTRODUCTION	1
II. VIGNETTING EFFECTS: SYSTEM GEOMETRY ONLY	2
III. VIGNETTING EFFECTS: SYSTEM GEOMETRY PLUS MIRROR REFLECTIVITIES	8
REFERENCES	18

I. INTRODUCTION

This report presents the results of a ray-trace analysis of the vignetting characteristics of the S-056 x-ray telescope. The present study was carried out under Contract No. NAS8-31996 by personnel of Montevallo Research Associates, Montevallo, Alabama during the period April 8, 1976 to April 30, 1976. Participating in the study were Dr. J. William Foreman, Jr. (Principal Investigator) and Mr. Joseph M. Cardone.

All computer runs were made in the double precision mode on the Univac 1110 digital computer located at the University of Alabama in Tuscaloosa, Alabama. Programs were entered and printouts were received from the Univac 1004 Remote Terminal located on the campus of the University of Montevallo in Montevallo, Alabama.

The object of the present study was to calculate the relative energy in the spot formed in the focal plane of the S-056 x-ray telescope by an off-axis point source at infinity for off-axis angles of 0, 1, 2, ..., 35 arc-minutes. At each off-axis angle, the relative energies were to be evaluated using theoretical x-ray reflectivity curves for wavelengths of 8.34 Å, 17.57 Å, and 27.39 Å, and also using an experimental x-ray reflectivity curve for 8.34 Å. The effects of vignetting due purely to the geometry of the S-056 optical system were to be evaluated separately, as well as jointly with the effects of mirror reflectivity.

II. VIGNETTING EFFECTS: SYSTEM GEOMETRY ONLY

In evaluating the vignetting effects due to system geometry only, the reflectivity at both mirrors of the x-ray telescope is taken to be unity, independent of the glancing angle of incidence at each mirror. The relative energy in the spot formed in the focal plane at each off-axis angle is then proportional to the number of rays reaching the focal plane, provided the same total number of rays is entered in the telescope aperture at each off-axis angle. Evaluation of the relative energy in the spot thus amounts to taking an inventory of all the rays traversing the system, keeping track of all the rays which eventually reach the focal plane. In order to fully understand vignetting effects, of course, one would also want to keep track of all the rays which do not reach the focal plane for various reasons.

The following factors will result in failure of a ray to reach the focal plane:

- (1) The ray fails to strike the parabolic mirror, but does strike the hyperbolic mirror. Such a ray will be intercepted by the second stop. It should be recalled that the second stop was designed to stop all rays which fail to strike both mirrors, and to pass all rays which do strike both mirrors over a field of view of ± 16 arc-minutes¹.
- (2) The ray strikes the parabolic mirror, but fails to strike the hyperbolic mirror. A ray of this type will also be intercepted by the second stop.
- (3) The ray fails to strike either mirror. No rays of this type were encountered in the present study, which covered a field of view of ± 35 arc-minutes.

(4) The ray strikes both mirrors, but is intercepted by the second stop.

Considering the design of the second stop, this should only begin to happen when an off-axis angle of 16 arc-minutes is reached or exceeded. This fact is confirmed by the present study.

In order to obtain a complete ray inventory, a total of 36,360 rays was entered in the telescope aperture at each off-axis angle and the ray-trace program was modified to keep track of the number of rays reaching the focal plane as well as the number of rays in each of the four categories listed above. The results are tabulated in Table I and presented graphically in Fig. 1.

A number of interesting observations can be made from the data in Table I and Fig. 1:

- (1) Even for the on-axis case, a large number of rays miss the parabolic mirror. This is because the outer radius of the front stop in the S-056 optical system is smaller than the minimum radius of the parabolic mirror. For the on-axis case, approximately 27% of the total number of rays entering the telescope aperture miss the parabolic mirror. This percentage remains nearly constant out to an off-axis angle of about 24 arc-minutes, where the number of rays missing the parabolic mirror begins to increase slowly with off-axis angle. At an off-axis angle of 35 arc-minutes, approximately 31% of the rays entering the aperture miss the parabolic mirror.
- (2) There is a practically linear vignetting of rays at the hyperbolic mirror as a function of off-axis angle. The hyperbolic mirror is just long enough to catch all the rays reflected from the parabolic mirror in the on-axis case. At an off-axis angle of 35 arc-minutes,

Table I. Vignetting ray inventory for S-056 as a function of off-axis angle.

Explanation of column headings:

MISSH: Total number of rays striking the parabolic mirror but missing the hyperbolic mirror.

MISSP: Total number of rays striking the hyperbolic mirror but missing the parabolic mirror.

HITPH: Total number of rays striking both mirrors.

STOP2: Total number of rays striking both mirrors but intercepted by the second stop.

NFOCAL: Total number of rays striking both mirrors and reaching the focal plane.

(NOTE: A total of 36,360 rays was traced at each off-axis angle.)

OFF-AXIS ANGLE (arc-min.)	MISSH	MISSP	HITPH	STOP2	NFOCAL
0	0	9,720	26,640	0	26,640
1	395	9,841	26,124	0	26,124
2	716	9,855	25,789	0	25,789
3	1,031	9,822	25,507	0	25,507
4	1,331	9,839	25,190	0	25,190
5	1,654	9,847	24,859	0	24,859
6	1,967	9,826	24,567	0	24,567
7	2,278	9,837	24,245	0	24,245
8	2,582	9,847	23,931	0	23,931
9	2,905	9,824	23,631	0	23,631
10	3,214	9,835	23,311	0	23,311
11	3,514	9,843	23,003	0	23,003
12	3,833	9,826	22,701	0	22,701

Table I. (Continued)

OFF-AXIS ANGLE (arc-min.)	MISSH	MISSP	HITPH	STOP2	NFOCAL
13	4,144	9,839	22,377	0	22,377
14	4,443	9,841	22,076	0	22,076
15	4,753	9,820	21,787	0	21,787
16	5,066	9,837	21,457	0	21,457
17	5,371	9,830	21,159	0	21,159
18	5,679	9,819	20,862	0	20,862
19	5,992	9,827	20,541	0	20,541
20	6,293	9,826	20,241	672	19,569
21	6,595	9,836	19,929	2,312	17,617
22	6,910	9,893	19,557	3,869	15,688
23	7,217	9,958	19,185	4,681	14,504
24	7,517	10,030	18,813	5,245	13,568
25	7,820	10,111	18,429	5,629	12,800
26	8,133	10,204	18,023	5,889	12,134
27	8,427	10,302	17,631	6,077	11,554
28	8,738	10,407	17,215	6,193	11,022
29	9,047	10,508	16,805	6,249	10,556
30	9,351	10,620	16,389	6,237	10,152
31	9,660	10,735	15,965	6,225	9,740
32	9,956	10,848	15,556	6,196	9,360
33	10,259	10,966	15,135	6,105	9,030
34	10,568	11,091	14,701	5,959	8,742
35	10,868	11,206	14,286	5,776	8,510

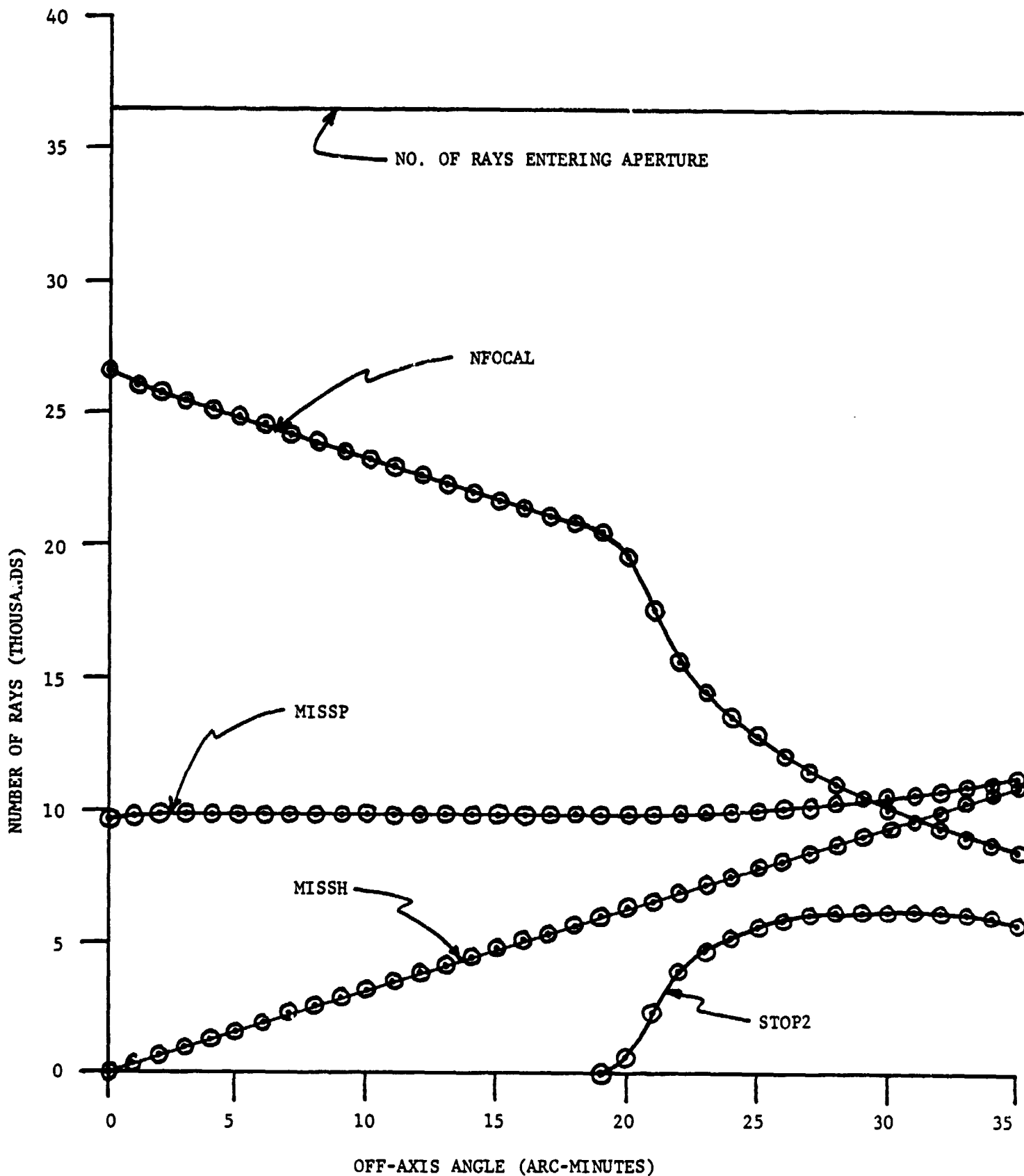


Figure 1. Graphical presentation of the ray inventory results for S-056.

10,868 rays which strike the parabolic mirror fail to strike the hyperbolic mirror; this represents about 30% of all the rays entering the aperture. It must be remembered, of course, that in designing the S-056 optical system Mangus and Underwood² investigated the tradeoff between hyperbolic mirror length and spot size in the focal plane as a function of off-axis angle. As the hyperbolic mirror is made longer to reduce off-axis vignetting at the hyperbolic mirror, the spot size in the focal plane increases, thereby degrading the angular resolution of the telescope.

- (3) The second stop does not begin to intercept any "good" rays (i.e., rays which have struck both mirrors) until an off-axis angle of 20 arc-minutes has been reached, at which point the second stop intercepts 672 out of the total of 20,241 good rays (this amounts to about 3% of the good rays). As the off-axis angle increases, the second stop intercepts more and more good rays, reaching a maximum of 6,249 intercepted out of a total of 10,556 good rays (about 59%) at an off-axis angle of 29 arc-minutes. At larger angles, the number of good rays intercepted by the second stop actually decreases slowly, apparently because of the steadily increasing vignetting at the hyperbolic mirror. Note, however, that the percentage of good rays intercepted by the second stop continues to increase, reaching a value of approximately 68% at an off-axis angle of 35 arc-minutes.

III. VIGNETTING EFFECTS: SYSTEM GEOMETRY PLUS MIRROR REFLECTIVITIES

The total vignetting produced by the S-056 optical system results not only from failure of some rays at each off-axis angle to reach the focal plane, but also from the fact that the reflectivity for x-rays at each mirror is less than unity. The x-ray reflectivity is a function of the glancing angle of incidence at each mirror, and in addition is strongly wavelength dependent. Three theoretical curves of reflectivity versus glancing angle of incidence for fused silica mirrors were furnished as input data for the present study³. These curves are for wavelengths of 8.34 Å, 17.57 Å, and 27.39 Å, respectively. In addition, some experimental data for reflectivity at 8.34 Å were furnished. The four reflectivity curves are shown in Fig. 2.

In order to compute the relative energy in the spot formed in the focal plane by an off-axis point source at infinity, a total of 36,360 rays was entered in the telescope aperture at each off-axis angle. The energy contribution from each ray which reached the focal plane was taken to be $R_p \cdot R_h$, where R_p and R_h are the reflectivities at the parabolic mirror and the hyperbolic mirror, respectively. The values of R_p and R_h were computed from the appropriate reflectivity curve in Fig. 2 using the glancing angles of incidence at the parabolic and hyperbolic mirrors which were calculated automatically for each ray as part of the ray-trace computer program. The resulting raw computer output data are summarized in Table II. For convenience, this table also lists the relative spot energy which would result from unit reflectivity for every ray. The numbers in this column are duplicates of the corresponding numbers in the

Table II. Raw computer data for S-056 vignetting including mirror reflectivity effects.

OFF-AXIS ANGLE (arc-min.)	Unit Reflectivity	RELATIVE ENERGY IN SPOT			8.34 Å (Exp.)
		8.34 Å	17.57 Å	27.39 Å	
0	26,640.0	15,576.3	16,802.6	21,911.0	8,173.3
1	26,124.0	15,258.8	16,477.7	21,486.9	7,986.3
2	25,789.0	14,997.5	16,266.5	21,211.6	7,801.8
3	25,507.0	14,724.2	16,088.4	20,979.7	7,600.2
4	25,190.0	14,388.7	15,887.5	20,717.7	7,368.2
5	24,859.0	13,998.7	15,677.5	20,442.3	7,116.6
6	24,567.0	13,565.2	15,491.7	20,196.1	6,858.3
7	24,245.0	13,047.6	15,286.5	19,922.2	6,581.7
8	23,931.0	12,488.7	15,085.9	19,653.7	6,295.1
9	23,631.0	11,895.9	14,894.0	19,396.2	6,010.3
10	23,311.0	11,248.4	14,689.0	19,122.1	5,727.5
11	23,003.0	10,566.9	14,491.3	18,857.8	5,461.2
12	22,701.0	9,890.4	14,297.1	18,598.5	5,213.6
13	22,377.0	9,238.9	14,088.9	18,321.4	4,970.4
14	22,076.0	8,655.9	13,894.8	18,063.8	4,740.5
15	21,787.0	8,136.4	13,708.2	17,817.3	4,523.2
16	21,457.0	7,646.2	13,495.4	17,540.3	4,314.4
17	21,159.0	7,204.3	13,302.2	17,292.1	4,126.5
18	20,862.0	6,804.6	13,109.0	17,046.5	3,946.8
19	20,541.0	6,444.6	12,899.6	16,782.3	3,774.0
20	19,569.0	6,054.3	12,283.6	15,988.3	3,552.0
21	17,617.0	5,617.9	11,060.2	14,396.6	3,261.9

Table II. (Continued)

OFF-AXIS ANGLE (arc-min.)	Unit Reflectivity	RELATIVE ENERGY IN SPOT			8.34 Å (Exp.)
		8.34 Å	17.57 Å	27.39 Å	
22	15,688.0	5,214.1	9,852.4	12,822.9	2,989.2
23	14,504.0	4,912.2	9,109.6	11,856.4	2,799.1
24	13,568.0	4,654.9	8,522.0	11,092.1	2,641.2
25	12,800.0	4,430.6	8,039.5	10,464.7	2,506.3
26	12,134.0	4,227.0	7,620.8	9,920.6	2,385.5
27	11,554.0	4,045.1	7,256.1	9,446.6	2,278.5
28	11,022.0	3,874.8	6,921.4	9,011.8	2,178.8
29	10,556.0	3,723.5	6,628.3	8,630.9	2,090.6
30	10,152.0	3,584.1	6,373.7	8,300.6	2,010.5
31	9,740.0	3,450.9	6,114.4	7,963.8	1,932.7
32	9,360.0	3,327.9	5,875.4	7,653.2	1,860.7
33	9,030.0	3,215.4	5,667.5	7,383.5	1,795.6
34	8,742.0	3,111.3	5,485.9	7,147.9	1,736.5
35	8,510.0	3,012.6	5,338.6	6,958.1	1,682.0

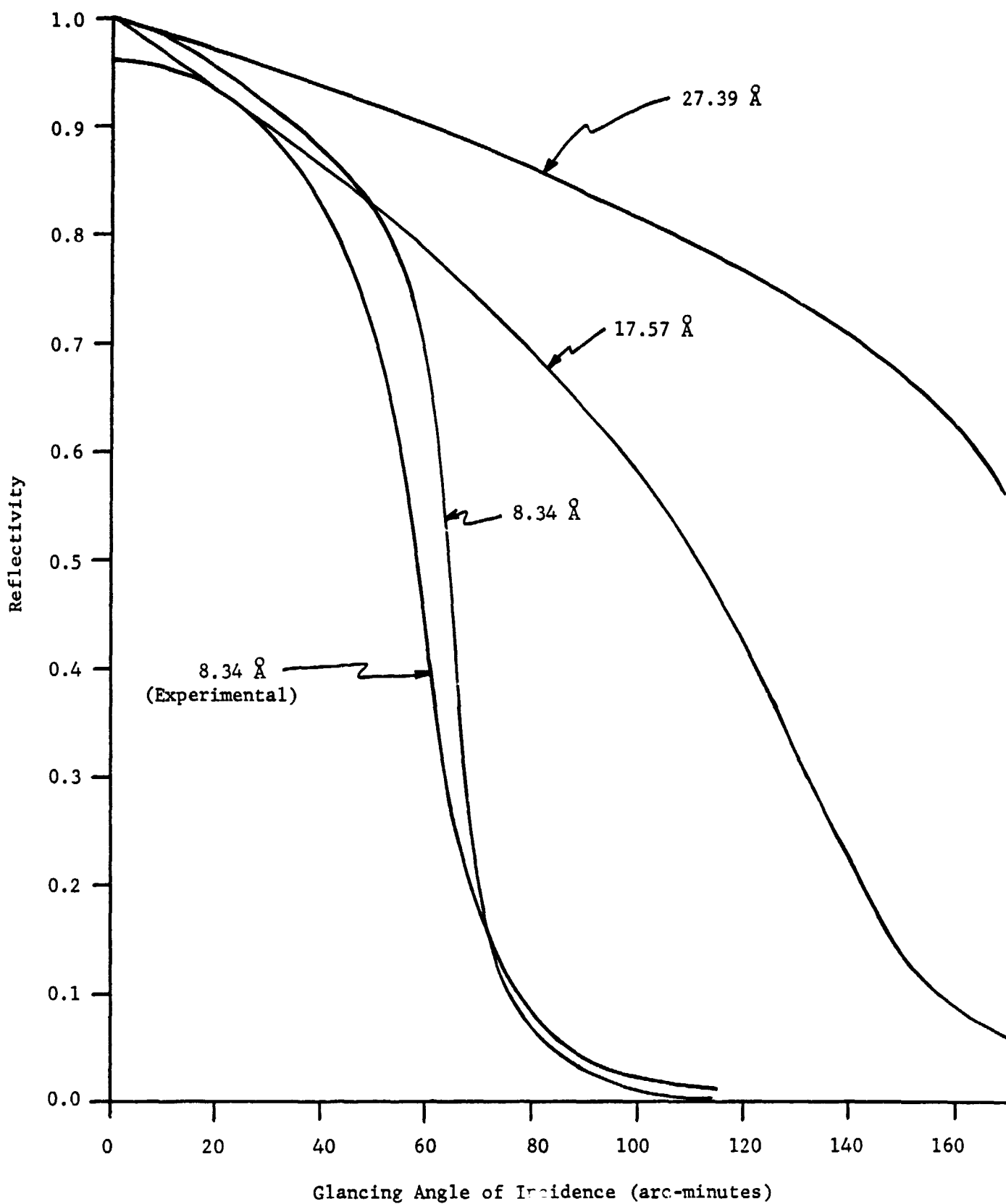


Figure 2. Theoretical x-ray reflectivity curves for wavelengths of 8.34 Å, 17.57 Å, and 27.39 Å. Also shown is an experimental reflectivity curve for 8.34 Å.

NFOCAL column in Table I.

In order to make the data in Table II more readily usable, it would be convenient to normalize all data to the relative energy for the on-axis case with unit reflectivity. This can be done by dividing every entry in Table II by 26,640.0. The resulting normalized relative energy data are summarized in Table III, and plotted in Fig. 3. Several observations are worthwhile with regard to these data:

- (1) When the actual mirror reflectivities are included in the relative energy calculation, there is a significant reduction in relative energy transmitted through the optical system of the S-056 x-ray telescope at any given off-axis angle, as expected. The relative energy in the spot increases with increasing wavelength, since the x-ray reflectivity curves fall off more slowly as a function of glancing angle of incidence at longer wavelengths, as shown in Fig. 2.
- (2) The second stop begins to play an obvious role in vignetting for off-axis angles greater than 20 arc-minutes for wavelengths of 17.57 Å and 27.39 Å. The effect of the second stop is far less obvious at a wavelength of 8.34 Å. Evidently those good rays at 8.34 Å which are intercepted by the second stop must strike the mirrors at such large glancing angles that their contribution to the relative spot energy is very small.
- (3) The vignetting curve using experimental reflectivity data at 8.34 Å lies significantly below the vignetting curve using theoretical reflectivity data at this wavelength. This is readily explained by the differences between the experimental and theoretical curves at 8.34 Å shown in Fig. 2. At small off-axis angles, the glancing angles of

Table III. Normalized vignetting data for S-056 including mirror reflectivity effects.

OFF-AXIS ANGLE (arc-min.)	Unit Reflectivity	RELATIVE ENERGY IN SPOT			8.34 Å (Exp.)
		8.34 Å	17.57 Å	27.39 Å	
0	1.0000	0.5847	0.6307	0.8225	0.3068
1	0.9806	0.5728	0.6185	0.8066	0.2998
2	0.9681	0.5630	0.6106	0.7962	0.2929
3	0.9575	0.5527	0.6039	0.7875	0.2853
4	0.9456	0.5401	0.5964	0.7777	0.2766
5	0.9331	0.5255	0.5885	0.7674	0.2671
6	0.9222	0.5092	0.5815	0.7581	0.2574
7	0.9109	0.4898	0.5738	0.7478	0.2471
8	0.8983	0.4688	0.5663	0.7377	0.2363
9	0.8870	0.4465	0.5591	0.7281	0.2256
10	0.8750	0.4222	0.5514	0.7178	0.2150
11	0.8635	0.3967	0.5440	0.7079	0.2050
12	0.8521	0.3713	0.5367	0.6981	0.1957
13	0.8400	0.3468	0.5289	0.6877	0.1866
14	0.8287	0.3249	0.5216	0.6781	0.1779
15	0.8178	0.3054	0.5146	0.6688	0.1698
16	0.8054	0.2870	0.5066	0.6584	0.1620
17	0.7943	0.2704	0.4993	0.6491	0.1549
18	0.7831	0.2554	0.4921	0.6399	0.1482
19	0.7711	0.2419	0.4842	0.6300	0.1417
20	0.7346	0.2273	0.4611	0.6002	0.1333
21	0.6613	0.2109	0.4152	0.5404	0.1224

Table III. (Continued)

OFF-AXIS ANGLE (arc-min.)	Unit Reflectivity	RELATIVE ENERGY IN SPOT			8.34 Å (Exp.)
		8.34 Å	17.57 Å	27.39 Å	
22	0.5889	0.1957	0.3698	0.4813	0.1122
23	0.5444	0.1844	0.3420	0.4451	0.1051
24	0.5093	0.1747	0.3199	0.4164	0.0991
25	0.4805	0.1663	0.3018	0.3928	0.0941
26	0.4555	0.1587	0.2861	0.3724	0.0895
27	0.4337	0.1518	0.2724	0.3546	0.0855
28	0.4137	0.1455	0.2598	0.3383	0.0818
29	0.3962	0.1398	0.2488	0.3240	0.0785
30	0.3811	0.1345	0.2393	0.3116	0.0755
31	0.3666	0.1295	0.2295	0.2989	0.0725
32	0.3514	0.1249	0.2205	0.2873	0.0698
33	0.3390	0.1207	0.2127	0.2772	0.0674
34	0.3282	0.1168	0.2059	0.2683	0.0652
35	0.3194	0.1131	0.2004	0.2612	0.0631

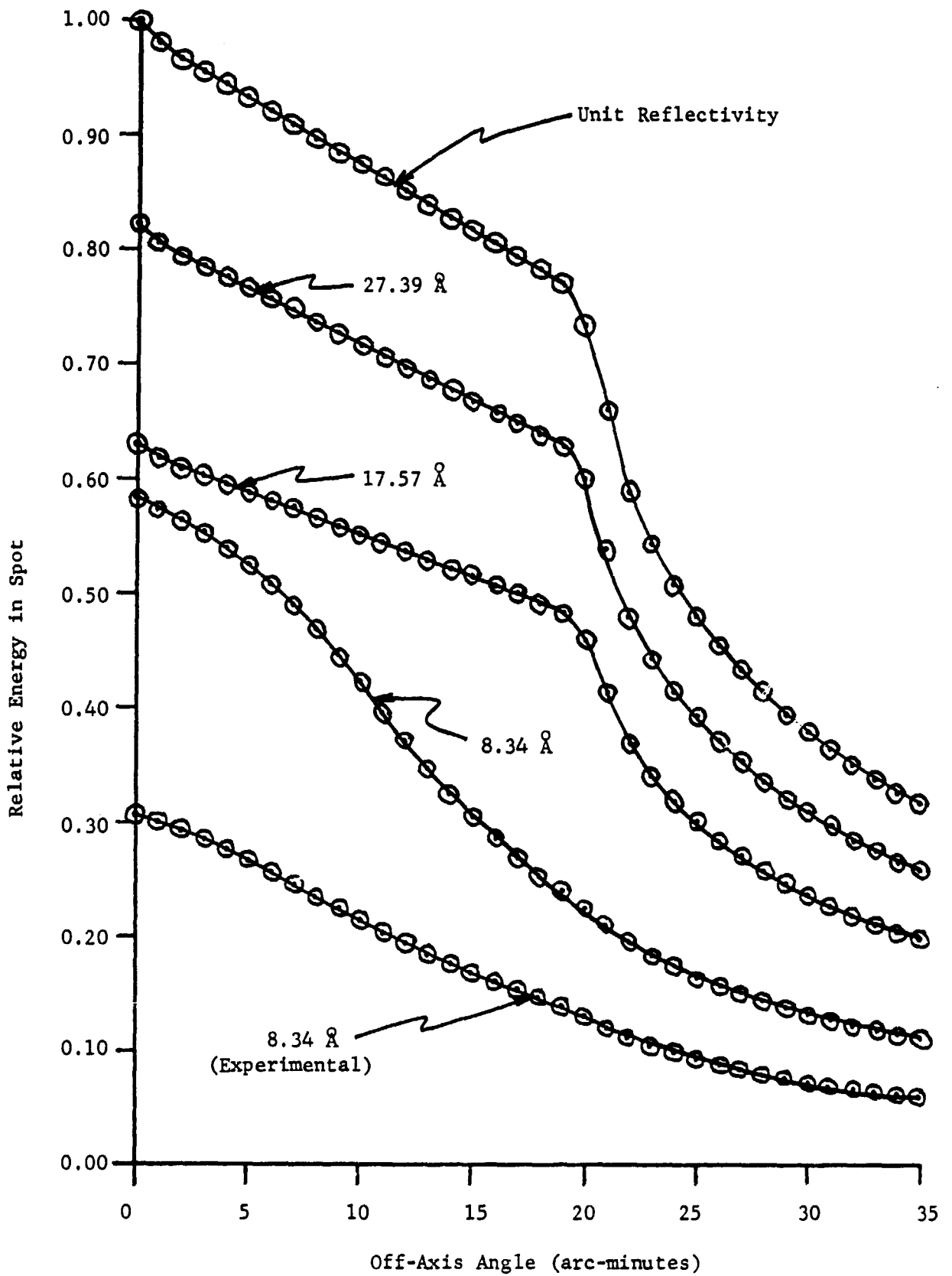


Figure 3. Normalized vignetting data for S-056 including mirror reflectivity effects.

incidence at both mirrors lie between 50 and 60 arc-minutes for all rays. Consider a ray, then, that has a glancing angle of incidence of 55 arc-minutes at each mirror. Using the theoretical x-ray reflectivity curve at 8.34 \AA shown in Fig. 2 then gives an overall reflectivity of $(0.775)^2 = 0.601$ for this ray. Using the experimental x-ray reflectivity curve at 8.34 \AA , on the other hand, gives an overall reflectivity of $(0.570)^2 = 0.325$. Thus, one would expect to find the relative spot energies roughly in the ratio $0.601/0.325 = 1.8$ at small off-axis angles. Looking at the actual data in Table III, one finds the relative spot energies in the on-axis case to be in the ratio $0.5847/0.3068 = 1.9$, which is very close to the rough estimate above. It may be concluded that if the experimental x-ray reflectivity data at 8.34 \AA is truly representative of the S-056 mirror reflectivities at 8.34 \AA as the telescope was used in orbit, then use of the theoretical x-ray reflectivity data at 8.34 \AA will lead to serious overestimation of the amount of energy actually reaching the film plane at any given off-axis angle. In the on-axis case, this overestimation will be roughly by a factor of 2.

In conclusion, it should perhaps be pointed out that the present study has obtained the relative energy in the entire spot formed in the focal plane of the S-056 x-ray telescope as a function of off-axis angle. Since the spot size increases with off-axis angle, the relative irradiance (energy per unit area) will fall off even faster than the total energy in the spot. In order to estimate the relative irradiance, it would be necessary to estimate the area of the spot at each off-axis angle and divide the relative energy by the relative spot area. This has not been done in the present study, but it would

not be a lengthy job given the data from the present report.

It is evident from the results presented here that a definitive statement about vignetting in the S-056 optical system could only be made if truly accurate reflectivity data were available. It appears from the 8.34 Å case studied here that the actual reflectivity data will lead to appreciably lower relative spot energies at a given off-axis angle than those obtained by use of theoretical reflectivity data.

REFERENCES

1. Foreman, Jr., J. W., G. H. Hunt, and E. K. Lawson. Analytical Study of the Imaging Characteristics of the Goddard ATM X-Ray Telescope, Report No. SP-505-0279, Space Support Division, Sperry Rand Corp., Huntsville, Alabama (September, 1969), pp. 40-48.

2. Mangus, J. D. and J. H. Underwood, Optical Design of a Glancing Incidence X-Ray Telescope, Applied Optics 8, 95(1969).

3. Neergaard, J. R., J. M. Reynolds, and S. A. Fields, The Theoretical Reflectance of X-Rays from Cu-K (1.54 \AA) to Be-K (113 \AA) Wavelengths, NASA TMX (to be published).